THE ASTROPHYSICAL JOURNAL, 238:585–595, 1980 June 1

INFRARED PHOTOMETRY OF SOUTHERN PLANETARY NEBULAE AND EMISSION-LINE OBJECTS

MARTIN COHEN[1,2]
NASA Ames Research Center, Moffett Field, California
AND
MICHAEL J. BARLOW[1]
Department of Physics and Astronomy, University College London
Received 1979 September 21; accepted 1979 December 4

ABSTRACT

Ten-micron photometry is presented of 23 planetary nebulae, seven very low excitation (VLE) nebulae, and 11 emission-line objects, of which more than half were also detected at 20 μm. The 10 μm behavior of the various classes of objects are compared, and it is shown that planetary nebulae can easily be distinguished from VLE nebulae by virtue of the silicate emission displayed by the latter. A uniform sample of planetary nebulae for statistical analysis is created by combining the present sample with our earlier northern hemisphere survey. It is shown that Lα photons are the dominant grain heating mechanism for nebular electron densities less than approximately 1.5×10^4 cm^{-3}, whereas above this density direct dust absorption of stellar continuum photons dominates.

Subject headings: infrared: sources — nebulae: planetary

I. INTRODUCTION

In this paper we present infrared observations of southern planetary nebulae and emission-line objects, which represent a continuation and extension of our earlier study of northern planetaries (Cohen and Barlow 1974, hereafter Paper I). The southern sky is rich in bright planetary nebulae, and the present investigation was intended both to enlarge the sample of objects for which radio and infrared properties could be compared and to survey for nebulae bright enough for subsequent study in the infrared at higher spectral resolution.

We have found it useful to separate the objects observed into three categories: (1) stellar emission-line objects of category D (Allen 1973), typified by hot dust emission apparent in the near-infrared; (2) bona fide planetary nebulae (PN); and (3) objects of very low excitation (VLE), defined by Sanduleak and Stephenson (1972) as having Hβ stronger than [O III] λ5007 and generally strong [O II] λ3727 emission. These authors exclude low-excitation nebulae which have Wolf-Rayet nuclei. In such a case, the Wolf-Rayet characteristics will dominate the optical spectrum. Recently Sanduleak and Phillip (1977) have shown that counterparts of the VLE objects in the Magellanic Clouds contain stars whose absolute magnitudes are typical of Population I objects (i.e., $M_V \approx -4$ to -5) so that the Galactic VLE objects may also represent a population different from that of planetary nebulae. It was our aim to determine whether these three categories of objects could be separated by their 10 μm infrared properties.

[1] Visting Astronomer, Cerro Tololo Inter-American Observatory, which is operated by the Association of Universities for Research in Astronomy, Inc., under contract with the National Science Foundation.

[2] NAS/NRC Senior Postdoctoral Associate.

II. OBSERVATIONS

a) *Infrared Observations*

All of the infrared observations were acquired using the CTIO 1.5 m telescope equipped with an f/30 chopping secondary and feeding a multifilter and multiaperture liquid-helium–cooled bolometer. We observed those nebulae whose optical diameters could be accommodated within 9″ or 18″ beams. Spatial chopping was used at a frequency of 21 Hz with throws of 15″ and 25″, respectively. Table 1 presents details of the filter system, the absolute flux calibration for zero magnitude, and self-consistent magnitudes for three standard stars. These standard magnitudes are based upon work by J. A. Frogel (1977, private communication) which was supplemented by us.

Table 2 summarizes our observations of the D-type emission-line objects, and Table 3 comprises those of both the planetary nebulae and the VLE objects, and the unclassified nebula He 2-77 (see § III*d*). Fluxes are given in janskys together with the ratios of mean to standard deviation of the mean, including all estimated errors, or 3 σ upper limits in the absence of detections. Fluxes measured with an 18″ beam are so indicated;

TABLE 1

THE INFRARED SYSTEM[a]

λ_{eff} (μm)	$\Delta\lambda$ (μm) FWHM	F_ν, Zero Mag (Jy)	α CMa	γ Cru	η Sgr
2.20	0.41	631	−1.39	−3.16	−1.51
3.45	0.57	294	−1.39	−3.36	−1.71
4.69	0.42	169	−1.39	−3.07	−1.42
8.0	0.6	62.0	−1.39	−3.27	−1.57
8.78	1.0	52.0	−1.39	−3.31	−1.61
9.78	0.9	42.2	−1.39	−3.37	−1.67
10	6	40.5	−1.39	−3.39	−1.67
10.60	1.8	36.3	−1.39	−3.41	−1.69
11.67	2.0	30.0	−1.39	−3.48	−1.75
12.69	1.3	25.6	−1.39	−3.49	−1.78
20	[b]	10.5	−1.39	−3.40	−1.80

[a] Effective wavelengths and FWHM of filters, fluxes for zero magnitude, and magnitudes for three standard stars.

[b] The 20 μm filter cuts on at about 15.5 μm and is cut off by the atmosphere at long wavelengths.

otherwise the measurements were made with a 9″ beam.

b) *Radio Observations*

We made high-frequency measurements of a handful of planetary nebulae using the NRAO[3] 11 m antenna in Tucson, Arizona. The dates of observation were 1976 October and 1977 January, and the frequencies were 31.4 and 90 GHz. In 1976 an uncooled, single channel, prime focus receiver was used at 31 GHz and a cooled, two channel, Cassegrain receiver was used at 90 GHz, each with a 6 Hz nutating subreflector. In 1977 we used a newly completed, uncooled, four channel Cassegrain system at 31 GHz with a 2.5 Hz nutating subreflector. This latter receiver provided much improved performance at the lower frequency over that used in 1976. Beams were 209″ (31 GHz) and 76″ (90 GHz) FWHM. Table 4 summarizes the results for seven nebulae. In all cases the results are consistent with optically thin free-free emission at both frequencies.

[3] The National Radio Astronomy Observatory is operated by Associated Universities, Inc., under contract with the National Science Foundation.

III. INFRARED FLUX DISTRIBUTIONS

a) *Stellar Emission-Line Objects*

In Figure 1 we present plots of the flux distributions of eight objects showing D-type emission according to Allen's (1973) criterion (hot dust emission apparent between 1 and 3 μm). We also include AG Car, a Be star in the center of a ring nebula which has been included in the PN catalog of Perek and Kohoutek (1967).

He 2-106 is a symbiotic star (Swings 1973). Its infrared flux distribution in the 8–13 μm region is consistent with a silicate emission feature superposed on a much broader continuum arising from thermal dust emission at a range of temperatures. The symbiotic star RR Tel also exhibits silicate emission in the 10 μm region (D. K. Aitken 1979, private communication).

The objects Ve 27, GG Car, He 2-80, He 2-90, and He 2-91 are all included in Allen and Swings's (1976) Group 2 category of peculiar Be stars in which the most numerous lines are those of permitted and forbidden ionized iron. Our 10 μm region coverage is insufficient for He 2-80 and He 2-91, but the flux

TABLE 2

OBSERVED FLUXES, F_ν (Jy), OF EMISSION-LINE OBJECTS[a]

	λ (μm)									
OBJECT	3.45	4.7	8.0	8.8	9.8	10	10.6	11.7	12.7	20
Ve 27	1.37 (13)	...	8.70 (6)	13.8 (32)	19.9 (36)	18.4 (45)	21.5 (48)	19.2 (83)	20.3 (83)	19.6 (7)
He 2-34	10.6 (70)	...	9.24 (10)	10.1 (25)	11.4 (22)	12.1 (50)	15.3 (66)	13.2 (25)	11.7 (23)	13.9 (4)
AG Car	4.10 (38)	3.96 (33)	...	1.89 (8)	...	1.65 (20)	...	1.14 (6)	...	<10.7
GG Car	10.2 (90)	11.5 (38)	9.85 (14)	10.6 (90)	11.0 (22)	10.5 (130)	10.6 (30)	9.05 (30)	7.73 (7)	<12.4
He 2-79	1.77 (25)	...	...	...	...	6.32 (70)	...	...	...	<35.7
He 2-80	...	...	...	...	...	6.19 (21)	...	...	...	4.63 (3)
He 2-90	2.81 (20)	12.1 (20)	33.9 (22)	35.6 (32)	34.3 (28)	45.9 (80)	27.8 (50)	25.0 (17)	53.3 (31)	68.1 (50)
He 2-91	4.70 (28)	6.75 (18)	...	7.50 (16)	...	6.45 (50)	...	5.24 (21)	...	3.71 (4)
He 2-106	13.9 (48)	17.3 (83)	18.7 (16)	25.2 (32)	31.1 (36)	27.6 (42)	33.4 (36)	29.0 (26)	29.4 (33)	17.4 (5)
CPD −56°8032	11.5 (70)	37.8 (200)	194 (130)	156 (140)	112 (50)	139 (48)	124 (160)	135 (400)	167 (110)	209 (140)

[a] Figures in parentheses following the fluxes represent the ratio of mean to standard deviation of the mean for each measurement.

TABLE 3

OBSERVED FLUXES, F_ν (Jy), OF PN, VLE, AND He 2-77

OBJECT	TYPE	λ (μm) 8.0	8.8	9.8	10	10.6	11.7	12.7	20
IC 418	PN	<2.64	3.59 (8)	5.43 (11)	10.0 (70)	9.98 (44)	12.6 (33)	19.2 (27)	30.0 (9)
NGC 2792[a]	PN	...	...	...	<0.33	...	...	...	...
NGC 2867[a]	PN	...	1.26 (5)	...	1.17 (7)	1.40 (6)	1.30 (5)	1.65 (3)	<10.1
IC 2501	PN	...	1.69 (8)	1.11 (4)	2.93 (24)	2.88 (15)	3.24 (12)	4.28 (6)	29.7 (5)
NGC 3132	PN	...	...	...	<0.34	...	...	...	...
He 2-47	VLE	<4.82	1.00 (6)	2.85 (4)	2.61 (19)	2.70 (8)	2.67 (10)	4.22 (6)	21.7 (8)
IC 2621	PN	2.72 (3)	2.65 (18)	2.22 (5)	3.84 (17)	4.70 (30)	5.29 (42)	7.05 (12)	16.2 (9)
NGC 3918[a]	PN	...	1.74 (14)	1.18 (4)	3.02 (31)	5.01 (20)	5.22 (18)	4.16 (7)	22.2 (4)
He 2-77	H II?	2.57 (4)	3.37 (15)	2.49 (6)	6.32 (23)	5.45 (10)	4.49 (12)	8.09 (13)	41.0 (22)
IC 4191	PN	...	0.82 (17)	...	1.22 (14)	2.52 (10)	2.46 (10)	<1.67	10.3 (4)
NGC 5189	PN	...	...	...	<0.31	...	...	...	...
NGC 5189[a]	PN	...	...	...	<0.38	...	...	...	...
He 2-99[a]	PN	...	...	...	0.66 (4)	...	...	...	7.82 (4)
NGC 5315	PN	...	...	...	4.93 (31)	...	...	...	25.4 (6)
NGC 5315[a]	PN	3.87 (4)	3.83 (13)	2.13 (9)	4.93 (19)	5.32 (22)	6.16 (26)	10.4 (17)	35.7 (7)
He 2-101	PN	...	...	...	<0.50	...	...	...	...
He 2-108[a]	VLE	...	...	...	<0.32	...	...	...	...
IC 4406[a]	PN	...	...	...	<0.34	...	...	...	...
NGC 5882	PN	...	...	...	1.10 (16)	...	...	...	6.27 (4)
He 2-131	VLE	<6.31	1.92 (8)	3.12 (11)	3.57 (37)	4.10 (11)	3.65 (43)	7.97 (24)	38.1 (20)
NGC 5979	PN	...	...	...	<0.34	...	...	...	...
He 2-138	VLE	...	0.76 (4)	...	1.29 (11)	...	1.21 (6)	2.48 (6)	21.2 (13)
NGC 6153[a]	PN	...	1.61 (14)	<1.22	2.76 (13)	6.00 (110)	4.92 (16)	<1.44	13.3 (4)
H 2-1	VLE	...	...	...	2.04 (12)	...	...	...	8.18 (4)
IC 4637[a]	PN	...	...	...	0.48 (3)	...	...	...	...
NGC 6369[a]	PN	...	0.82 (4)	...	1.65 (8)	2.36 (9)	2.46 (17)	...	<11.9
He 2-260	VLE	...	...	...	<0.41	...	...	...	...
Tc 1[a]	VLE	...	...	...	1.00 (7)	...	0.89 (5)	...	<15.3
Hb 5[a]	PN	10.5 (12)	5.45 (17)	2.81 (7)	6.50 (30)	6.62 (17)	7.75 (25)	9.86 (26)	21.7 (8)
NGC 6537[a]	PN	2.92 (5)	2.56 (12)	1.46 (5)	3.63 (33)	4.57 (17)	4.20 (19)	4.00 (10)	21.2 (7)
M 1-38	PN	...	...	...	<0.43	...	...	...	...
NGC 6567	PN	2.44 (3)	1.42 (6)	1.05 (3)	1.96 (15)	2.29 (13)	2.00 (9)	2.67 (6)	31.4 (3)
NGC 6578	PN	...	...	...	0.66 (7)	...	...	...	3.77 (4)

[a] Denotes measurement with 18″ beams; all other observations with 9″. Figures in parentheses as in Table 2.

distributions of GG Car and Ve 27 again indicate silicate emission in the 10 μm region. The flux distribution of He 2-90 is more baffling, since the five data points between 8.0 and 11.7 μm define a smooth and self-consistent spectrum, compared with which we can only suggest that the greatly elevated 12.7 μm point is due to [Ne II] emission. Moreover, the slope of the flux distribution between 4.7 and 11.7 μm is too sharply peaked to be a blackbody. Therefore it may be necessary to invoke some nongray grain material whose identity is as yet unknown.

He 2-34 is classified as a suspected VLE object by Sanduleak and Stephenson (1973). A rather broad feature occurs between 8 and 13 μm, characterized by a peak at 10.6 μm not readily identifiable as silicate emission, which should peak at 9.8 μm. It is conceivable that the peak could include [S IV] emission at 10.5 μm. However, [S IV] line emission cannot explain the rather smooth, broad emission peak which is observed and which does not correspond to any resonant emission feature known to occur in other astronomical objects. Nor should a low excitation nebula display the [S IV] ion.

CPD $-56°8032$ has been classified as type WC10 by Webster and Glass (1974). The most obvious initial interpretation of the trough in the spectrum centered at 9.8 μm would be silicate absorption. The optical depth implied for this feature would then be $\tau_{sil} \sim 0.5$, which for "normal" ratios of A_V/τ_{sil} (Rieke 1974; Gillett *et al.* 1975) would suggest an A_V of about 8 mag. However, the $(V-K)$ index of 4.3 for this object provides a rigid upper limit of $A_V < 5$. Moreover, this limit is clearly too high because of obvious thermal dust emission at 2.2 μm. Optical spectrophotometry of CPD $-56°8032$ which we have acquired yields $A_V = 1.85$, where the narrow Hα and Hβ lines are assumed to originate

TABLE 4

HIGH-FREQUENCY RADIO MEASUREMENTS

Nebula	S(31.4 GHz) (mJy)	S(90 GHz) (mJy)
IC 3568	141 ± 30	...
NGC 6537	396 ± 103	283 ± 89
NGC 6572	1146 ± 223	...
NGC 7009	631 ± 154	...
BD +30°3639	616 ± 82	519 ± 165
M 1-78	1000 ± 66	909 ± 190
IC 5117	408 ± 54	321 ± 90

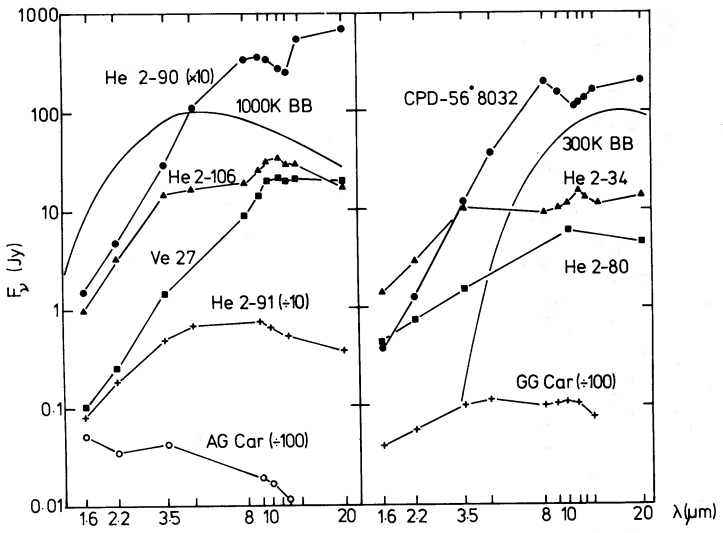

FIG. 1.—The infrared flux distributions of nine emission-line objects. Two blackbody curves are shown for comparison.

under case (*b*) conditions in the same region as the narrow nebular forbidden lines, rather than from the circumstellar region giving rise to the broader permitted line spectrum. In addition to these objections to the silicate absorption hypothesis, it is most improbable that oxygen-rich silicate grains could condense around this carbon-rich WC star. A more plausible interpretation of the shape of the spectrum of CPD −56°8032 in the 10 μm region is that it is similar to the *continuum* flux distribution of NGC 7027, in particular having a strong 7.7 μm feature (see the composite spectrum of NGC 7027 in Fig. 1 of Russell, Soifer, and Willner 1977).

AG Car shows an excess between 2.2 and 11.7 μm attributable to free-free emission, and the IR flux distribution is similar to that found for Population I Be stars by Gehrz, Hackwell, and Jones (1974). The steepening of the excess free-free spectrum at longer infrared wavelengths can be interpreted as due to emission from an optically thick wind having an approximately inverse-square law density distribution (Wright and Barlow 1975). There is no evidence for thermal dust emission from AG Car. We believe that there is no justification for the classification of AG Car and its associated ring nebula (of diameter some 36″) as a planetary nebula.

All of the other objects plotted in Figure 1 have infrared flux distributions radically different from that of AG Car, in the sense that they all show strong dust emission.

b) Planetary Nebulae

Figure 2 illustrates the flux distributions observed for 12 PN. Apart from IC 418, all of the planetaries for which narrowband 9.8 μm data exist show deep troughs at this wavelength. However, we do not interpret this phenomenon in terms of absorption by silicate dust, for basically the same reason as given in the discussion of CPD −56°8032 above. In the present context the discrepancy between the expected values of A_V as deduced from the optical depth of the putative silicate features, versus the total extinction at Hβ deduced by Milne and Aller (1975) using the radio-Hβ method, is enormous (e.g., 10–30 mag expected, compared with 0.8–3.5 mag observed).

Instead we regard the 9.8 μm point as the most representative of the true continuum, whereas each of the other five narrow-band filters potentially includes an emission line or feature known to occur in planetary nebulae. The λ8.0 filter can include the strong, broad 7.7 μm feature found in NGC 7027 by Russell, Soifer, and Willner (1977). The λ8.8 filter can include the long wavelength wing of this 7.7 μm feature, together with the 9.0 μm [Ar III] line and the 8.7 μm feature seen by Gillett, Forrest, and Merrill (1973) in NGC 7027. The λ10.6 filter can include the 10.5 μm [S IV] line as well as the edge of the 11.3 μm feature found by Gillett, Forrest and Merrill (1973). The λ11.7 filter fully brackets this latter feature. The λ12.7 filter can include the 12.8 μm [Ne II] line. Finally, Willner *et al.* (1979) have established the presence in IC 418 of a broad feature between 10 and 14 μm, which they attribute to silicon carbide emission. It is possible that in all planetary nebulae this feature underlies the narrower lines and features. Our observed flux distribution for IC 418 (Fig. 2) agrees very well with the spectrophotometry of Willner *et al.*, although our absolute fluxes are lower, due to the use of a smaller aperture.

If we examine the steepness of the decline of the flux distributions between 8.0 and 9.8 μm, it is clear that we may order the well-observed planetaries in the following sequence: Hb 5, NGC 6537, NGC 5315, IC 2501, NGC 3918, NGC 6567, IC 2621, and IC 418. This sequence may be interpretable as one of diminishing strength of the 7.7 and 8.7 μm features relative to a

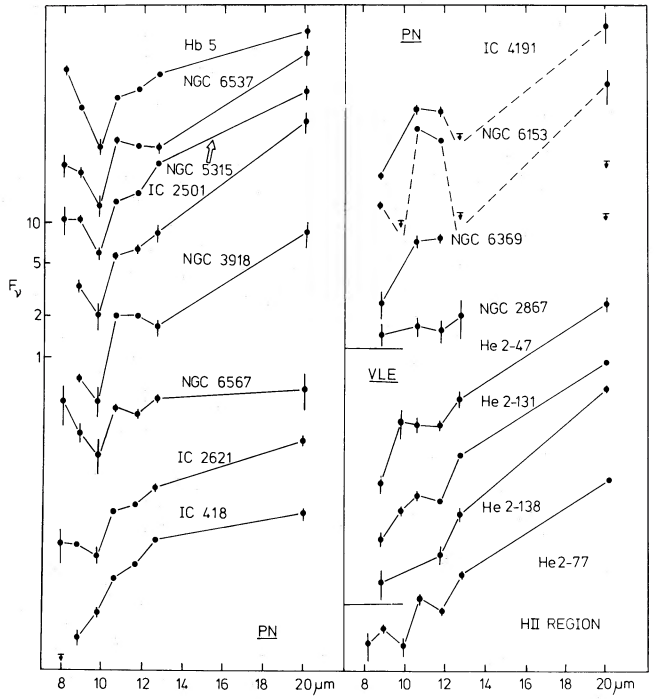

FIG. 2.—The 8–20 μm flux distributions of 12 planetary nebulae, three VLE nebulae, and the possible H II region He 2-77

general underlying continuum. No 9.8 μm flux point exists for IC 4191, NGC 6369, or NGC 2867, but a trough at 9.8 μm definitely exists for NGC 6153. The data for IC 4191 and NGC 6153 are particularly striking in that both show remarkably strong emission at 10.6 and 11.7 μm compared with the severe upper limits to adjacent narrow-band fluxes. These elevated fluxes might represent [S IV] and broad 11.3 μm emission, respectively. One might then predict both 7.7 and 11.3 μm features at high resolution.

c) *Very Low Excitation Objects*

The 10 μm flux distributions of the VLE objects He 2-47, He 2-131, and He 2-138 (Sanduleak and Stephenson 1972) are plotted in Figure 2. They differ in an obvious way from bona fide planetaries in that the flux at 8.8 μm is much lower than that at 9.8 μm. We interpret the flux distribution of He 2-47 as being due to silicate emission peaking at 9.8 μm, along with strong [Ne II] emission at 12.8 μm. The flux distribution of He 2-131 (and presumably He 2-138) is also interpreted in the same manner. Aitken *et al.* (1979) have obtained spectrophotometry of the VLE object M 1-26 and found that it also exhibits silicate emission and a strong [Ne II] line. Aitken *et al.* also have found silicate emission in the spectrum of SwSt 1 (HD 167362) whose nucleus is classified by Smith and Aller (1969) as transitional between Wolf-Rayet and Of types. Comparison of our own (unpublished) optical spectra, taken with the Lick image-tube scanner at the 3 m telescope, of SwSt 1 and BD +30°3639 supports their view. The spectrum of BD +30°3639 is conspicuously that of a cool WC type nucleus, with a rich broad-lined spectrum of C III and C IV in addition to the nebular lines. By contrast, SwSt 1 shows only a few of the strongest carbon lines in emission, principally $\lambda\lambda$4650 and 5696 of C III. These, and other lines, are significantly narrower than the corresponding lines seen for BD +30°3639, as would be expected for an Of type nucleus (cf. Smith and Aller 1969). SwSt 1 reveals dominantly the spectrum of a VLE object. We feel that BD +30°3639 is definitely a PN, but that SwSt 1 is an object on the borderline between PN and VLE objects, albeit closer to the latter. Therefore, VLE objects can be immediately distinguished from PN on the basis of their 10 μm flux distributions, and it would appear that VLE objects are oxygen-rich whereas PN are carbon-rich. This supposition has been verified by observations of He 2-131 with *IUE* by M. J. Seaton (1979, private communication), showing that O/C > 1 in this object. The evolutionary status of the VLE objects remains to be understood.

d) *He 2-77*

He 2-77 is included in the catalog of Perek and Kohoutek (1967) and its 10 μm flux distribution (Fig. 2) resembles that of planetary nebulae, showing a dip at 9.8 μm. However, morphologically He 2-77 has a patchy, irregular shape with no obvious central star and moreover has a rather large 5 GHz radio flux of 2.3 Jy (Milne 1979). We have acquired optical spectrophotometry of He 2-77 which shows it to be heavily

obscured. An analysis of the observed Hα/Hβ ratio, assuming case (*b*) conditions to hold, yields $A_V = 8.9$ mag. This would predict an optical depth at 10 μm, due to silicate absorption, of $\tau_{sil} \sim 0.6$, consistent with the observed dip at 9.8 μm. The observed elevation of the adjacent 8.8 and 10.6 μm flux points would have to be ascribed to line emission by [Ar III] and [S IV], respectively, under this hypothesis. We should emphasize that He 2-77 is the only object in our sample for which the 9.8 μm trough is consistent with silicate absorption. We therefore suggest that He 2-77 is a heavily obscured compact H II region. Radio observations in search of an associated molecular cloud would be very useful.

IV. NEBULAR PARAMETERS AND HEATING MECHANISMS

By combining the present IR photometry with that from Paper I, we have created a sample of PN for further analysis. To be included in the sample, a nebula had to satisfy the following conditions: (1) both 10 and 20 μm data had to be available; (2) the nebula must have been observed with apertures larger than its optical diameter; (3) the nebula could not be a VLE object since these are known, following the discussion in § III*c*, to show infrared properties radically different from those of PN.

In addition to the nebulae excluded by the above criteria, the nebulae HD 167362, Vy 2-2, and Hb 12 were also excluded. These three objects are known to have a steep radio spectral index, indicative of an r^{-2} density distribution (Marsh, Purton, and Feldman 1976). Since their radio emission is optically thick, an estimate cannot be made of their Lα luminosities. Aitken *et al.* (1979) have found that SwSt 1 and Hb 12 exhibit silicate emission in the 10 μm region. In addition, Allen and Swings (1976) have found that Hb 12 has a WN type nucleus, in contrast to the WC type classification always appropriate for Wolf-Rayet central stars of planetary nebulae.

We are left with 30 PN, for which we have derived various parameters. The method used here to derive grain temperatures from our 10 and 20 μm data differs from that of Paper I in two ways. (1) In Paper I we assumed that the grains emitted as blackbodies. It is more realistic to assume a λ^{-2} emissivity dependence for grains emitting in the infrared continuum (e.g., as assumed by Telesco and Harper (1977) and by McCarthy, Forrest, and Houck (1978)). The effect of including this dependence is to lower the derived temperatures. (2) Broad-band 10 μm fluxes were used in Paper I. A comparison of the broadband 10 μm and narrowband 9.8 μm data for the PN data in Table 3 shows that the broad-band fluxes seriously overestimate the true level of the continuum at 10 μm, due to the inclusion of numerous strong emission lines and features in the bandpass, as discussed in § III*b*. For the eight nebulae on the left-hand side of Figure 2, the ratio of broad-band 10 μm flux to narrow-band 9.8 μm flux has a fairly narrow range, with a mean value of 2.3 ± 0.4. For those nebulae not possessing 9.8 μm photometry we have constructed 9.8 μm fluxes by dividing their broad-band 10 μm fluxes by this factor. For a number of nebulae, 9.8 μm fluxes could be obtained from published IR spectrophotometry. These include NGC 7027 and BD +30°3639 from Gillett, Forrest, and Merrill (1973), IC 418 and NGC 6572 from Willner *et al.* (1979), NGC 6790 from Aitken *et al.* (1979), and IC 5117 and NGC 6302 from Grasdalen (1979: the flux for NGC 6302 was scaled to the total 10 μm flux of Danziger, Frogel, and Persson 1973). The effect of using narrow-band instead of broad-band 10 μm fluxes is again to lower the derived 10–20 μm grain temperatures.

For the case of NGC 7027, a λ^{-2} grain emissivity applied to the 9.8 and 20 μm fluxes (the latter from Becklin, Neugebauer, and Wynn-Williams 1973) yields a grain temperature of 139 K, compared with a grain temperature of 90–95 K derived from the longer wavelength fluxes by Telesco and Harper (1977) and by McCarthy, Forrest, and Houck (1978). One possibility for this discrepancy is that the 9.8 μm measurements do not really sample the "true" underlying continuum but instead merely represent the intersection of the wings of the 7.7 μm and a combination of the 11.3 μm and silicon carbide features. However, Figure 3 of McCarthy, Forrest, and Houck (1978) shows that fitting the $\lambda > 25$ μm data for NGC 7027 with 90 K grain emission leaves an excess of smooth continuum shortward of 20 μm, thereby establishing the existence of a range of dust temperatures. We shall therefore assume that our data give a meaningful representation of the underlying continuum at 9.8 μm.

In Paper I we used the distance scale of Higgs (1971) to derive nebular luminosities. However, that distance scale assumes the same ionized mass for all nebulae and therefore can seriously overestimate the distances of nebulae which are optically thick in the Lyman continuum. Consequently, in this paper, we shall adopt the distance scale of Acker (1978), which allows for this effect. We have derived nebular Lα luminosities from the 5 GHz fluxes of Milne and Aller (1975) and Milne (1979), using the method of Rubin (1968) and an assumed mean nebular electron temperature of $T_e = 12{,}000$ K. Infrared luminosities have been calculated solely on the basis of the energy emitted by grains with a λ^{-2} emissivity, normalized to the 9.8 and 20 μm fluxes. These IR luminosities thus do not allow for cooler grains emitting at longer wavelengths, as discussed below.

Table 5 lists the various derived nebular parameters. Column (1) gives the names of the nebulae in right ascension order, column (2) lists the 9.8 μm fluxes (in parentheses if derived from broadband 10 μm fluxes), column (3) gives the 9.8–20 μm (or 9.8–18 μm for nebulae from Paper I) grain temperatures T_d, column (4) lists the 5 GHz radio fluxes, column (5) gives the distances D (in kpc), and columns (6) and (7) list the Lα and infrared luminosities $L_{L\alpha}$ and L_{IR}, in units of solar luminosities. Column (8) gives the ratio $L_{IR}/L_{L\alpha}$ for

TABLE 5

NEBULAR PARAMETERS

Nebula	F_ν (9.8 μm) (Jy)	T_d (9.8–20) (K)	F_ν (5 GHz) (Jy)	D (kpc)	$L_{L\alpha}$ ($L_\odot$)	L_{IR}[a] ($L_\odot$)	$L_{IR}/L_{L\alpha}$	n_e (FL) (cm^{-3})	n_e (rms) (cm^{-3})
IC 418	17.6	142	1.613	0.36	74	68	0.91	18000	14000
IC 2149	(0.45)	118	0.254	1.0	94	36	0.39	3000	6000
IC 2165	(0.34)	122	0.188	3.1	573	216	0.38	3000	8000
J900	(1.08)	124	0.121	2.25	192	326	1.70	...	4000
IC 2501	1.11	108	0.261	1.3	164	281	1.71	...	...
IC 2621	2.22	135	0.195	1.1	88	101	1.15	...	8000
NGC 3918	1.18	116	0.859	0.8	190	68	0.36	2000	7000
IC 4191	(0.55)	114	0.172	2.25	323	282	0.87	...	...
NGC 5315	2.13	117	0.476	2.8	1387	1422	1.03	...	...
NGC 5882	(0.50)	122	0.370	1.9	496	118	0.24	...	9000
IC 4593	(0.33)	107	0.104	1.95	147	200	1.36	2000	2000
NGC 6210	(0.86)	117	0.311	1.05	126	81	0.64	6000	2500
IC 4634	(0.31)	107	0.129	2.9	399	424	1.06	...	3000
NGC 6302	10.4	115	3.49	0.65	421	420	1.00	7000	6000
Hb 5	2.81	134	0.548	1.9	736	396	0.54	...	...
NGC 6537	1.44	120	0.671	1.24	277	160	0.58	4000	10000
NGC 6572	11.1	122	1.307	0.67	213	325	1.53	9000	8000
NGC 6567	1.05	144	0.176	1.2	92	42	0.46	3000	4000
NGC 6578	(0.30)	122	0.170	2.9	532	165	0.31	...	3000
Hu 2-1	(0.99)	126	0.130	1.3	82	91	1.10	9000	13000
NGC 6741	(0.72)	128	0.220	1.6	182	91	0.50	3000	12000
NGC 6790	5.41	139	0.256	1.6	225	454	2.02	20000	37000
NGC 6803	(0.60)	123	0.114	1.6	109	95	0.87	5000	4000
NGC 6807	(0.45)	120	0.022	5.1	168	851	5.07	...	13000
BD +30°3639	48.7	142	0.511	0.65	116	613	5.28	7000	15000
NGC 6881	(0.86)	126	0.183	3.6	881	604	0.69	...	11000
NGC 6884	(0.38)	128	0.171	2.8	498	146	0.29	9000	7000
NGC 6886	(0.39)	113	0.105	3.1	344	408	1.19	5000	10000
NGC 7027	135	139	6.28	1.09	2773	5257	1.90	20000	26000
IC 5117	6.34	136	0.230	2.2	380	1114	2.93	...	30000

[a] See text, § IV.

each nebula. Column (9) lists the electron densities of the nebulae n_e(FL) derived from the [O II] line ratios and nebular temperatures collected by Sabbadin and Minello (1978). These are distance-independent. Column (10) lists the rms electron densities n_e (rms) derived by Higgs (1971). These are model-dependent, and assume $T_e = 12{,}000$ K.

For one nebula, NGC 7027, the infrared flux has been measured over a wide enough wavelength range to allow the total infrared luminosity to be evaluated. Telesco and Harper (1977) found a total infrared flux of 2.4×10^{-10} W m^{-2}, distributed such that one third was emitted in each of the intervals 1–17 μm, 17–30 μm, and 30–300 μm. The ratio of total infrared to Lα luminosity is 3.15 (this differs from the ratio of 3.6 deduced by Telesco and Harper due to the fact that the latter authors adopted a higher nebular electron temperature of 15,000 K when calculating $L_{L\alpha}$). The estimate of L_{IR} for NGC 7027 in Table 5, produced solely by fitting a 139 K λ^{-2} emissivity blackbody to the 9.8 and 20 μm fluxes, accounts for 60% of the *total* infrared flux. Of the remainder, 8% is emitted by emission features and hotter dust at shorter wavelengths and 32% is emitted by cooler dust at longer wavelengths. Another way of looking at this is to say that a 90 K λ^{-2} emissivity blackbody fitted to the 30 μm flux accounts for 73% of the total infrared flux, with the remainder emitted by hotter dust at shorter wavelengths. Undoubtedly a range of grain temperatures is present, which can most easily be explained by a range of grain sizes (Panagia, Bussoletti, and Blanco 1977; Mathis 1978). The point to be made here is that although far-infrared flux measurements are required for a definitive discussion of the infrared properties of planetary nebulae, the estimates of L_{IR} in Table 5 probably represent about 60% of the total infrared luminosity, thereby allowing a discussion of the *relative* IR properties of planetaries.

Telesco and Harper (1977) have shown that absorption by dust of diffuse nebular radiation, including Lα, can lead to values of $L_{IR}/L_{L\alpha}$ in excess of unity without the need for direct absorption of stellar Lyman continuum photons by the dust. However, a ratio of $L_{IR}/L_{L\alpha} > 3$, such as NGC 7027 possesses, must indicate significant dust absorption of Lyman continuum photons, since complete absorption of all diffuse radiation unaccompanied by direct absorption of stellar photons is an unlikely scenario. A detailed analysis of NGC 7027 by Panagia, Bussoletti, and Blanco (1977) led to an estimate of a dust optical depth to Lyman continuum photons of $\tau_{UV} \approx 0.3$. We shall take the view that the nebulae in Table 5 with values of $L_{IR}/L_{L\alpha}$ greater than or equal to that of NGC 7027 definitely experience significant dust absorption of

stellar continuum photons. These nebulae are NGC 6790, NGC 6807, IC 5117, and BD +30°3639 (as discussed in Paper I, the central star of the last nebula is so cool that dust absorption of stellar photons emitted *longward* of the Lyman continuum is probably the dominant mechanism powering the infrared flux. Our high-frequency radio data for BD +30°3639 support the view expressed by O'Dell and Terzian 1970, that the 5 GHz radio flux of this object is not optically thin.) Of the remaining 25 nebulae in Table 5, only two (J900 and IC 2501) have values of $L_{IR}/L_{L\alpha}$ approaching that of NGC 7027, so that some absorption of Lyman continuum photons may be indicated. The remainder possess values of $L_{IR}/L_{L\alpha}$ comfortably close to or lower than unity such that the dominant grain heating source may be supposed to be Lα photons.

As a test of the Lα heating hypothesis, 9.8 μm infrared fluxes may be plotted versus 5 GHz radio fluxes. Radio free-free fluxes are proportional to the product of nebular electron and ion densities, as are Lα fluxes. Therefore we should expect a linear relationship between 9.8 μm and 5 GHz fluxes if Lα predominantly powers the infrared emission. In Paper I we plotted *absolute* infrared and radio properties. Grasdalen (1979) has criticized this procedure, on the grounds that the introduction of distances artificially stretches the plots and produces a spurious relationship between quantities. To test this hypothesis, we have plotted in Figures 3*a* and 3*b*, respectively, the observed fluxes and the absolute fluxes. Inspection of the diagrams shows that the introduction of absolute quantities does not stretch the range of values plotted, the range in fact being smaller for the absolute quantities. There is, however, evidence that the introduction of absolute values has weakened the correlation between 9.8 μm and 5 GHz fluxes, presumably because of inaccuracies in the distance scale. With the omission of the five nebulae for which significant dust absorption of stellar photons is indicated (those with tick marks in Figs. 3*a*

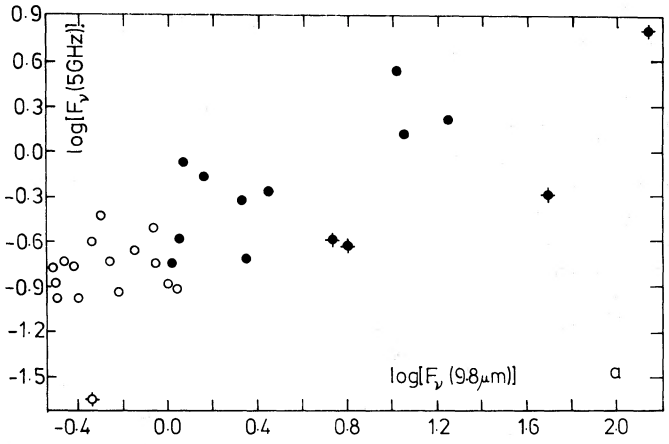

FIG. 3*a*

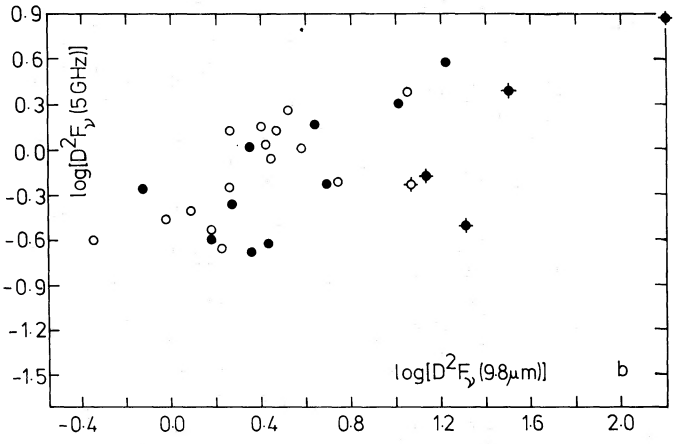

FIG. 3*b*

FIG. 3.—(*a*) The apparent 9.8 μm fluxes plotted against the apparent 5 GHz fluxes of 30 planetary nebulae. The filled circles represent nebulae whose 9.8 μm flux has been measured directly, and the open circles represent nebulae whose 9.8 μm flux has been estimated from their broad-band 10 μm flux, as described in the text. The tick marks on symbols denote nebulae whose values of $L_{IR}/L_{L\alpha}$ in Table 5 indicate that dust absorption of stellar continuum photons is important. These nebulae are (from left to right) NGC 6807, NGC 6790, IC 5117, BD +30°3639, and NGC 7027. (*b*) Same as Fig. 3*a*, but for *absolute* fluxes, where D is the distance of a nebula, in kpc.

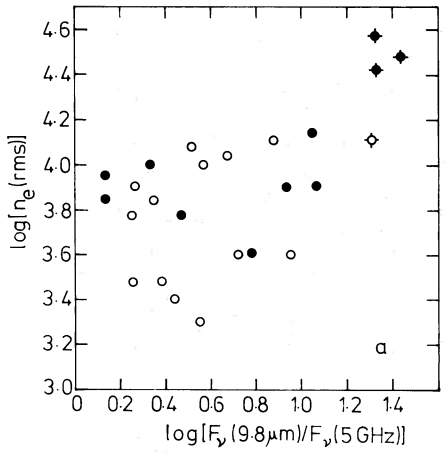

FIG. 4a

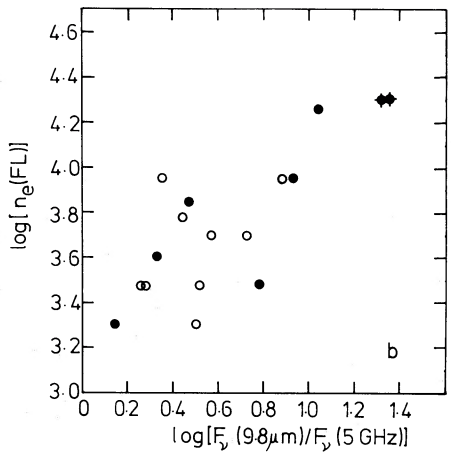

FIG. 4b

FIG. 4.—(*a*) The ratios of the 9.8 μm and the 5 GHz fluxes of 25 planetary nebulae plotted against their rms electron densities, taken from Higgs (1971). Symbols as in Fig. 3. (*b*) The ratios of the 9.8 μm and 5 GHz fluxes plotted against the electron densities of planetary nebulae deduced from the forbidden line ratios of [O II] λλ3726, 3729.

and 3*b*), the following least-squares fits are obtained for the remaining 25 nebulae:

$$\log \{F_\nu(9.8\ \mu\text{m})\} = 0.57 + 1.01 \log \{F_\nu(5\ \text{GHz})\} \quad (1)$$

with a correlation coefficient $r^2 = 0.69$; and

$$\log \{D^2 F_\nu(9.8\ \mu\text{m})\} = 0.52 + 0.70 \log \{D^2 F_\nu(5\ \text{GHz})\} \quad (2)$$

with a correlation coefficient $r^2 = 0.50$.[4] We propose that relationship (1), in conjunction with the $L_{IR}/L_{L\alpha}$ ratios in Table 5, provides strong evidence that Lα photons are the dominant grain heating mechanism in the majority of planetary nebulae.

Grasdalen (1979) has suggested that a more important correlation exists, between nebular electron density and the ratio of 10 μm to radio flux. He goes on to argue from this that direct absorption of stellar continuum photons is the dominant heating mechanism in planetary nebulae. In Figure 4*a* we present the equivalent diagram to Figure 2 of Grasdalen (1979), where we have plotted the ratio of 9.8 μm and 5 GHz fluxes against the rms electron density taken from Higgs (1971; these densities, listed in col. [10] of Table 5, are the same as those used in Paper I and by Grasdalen). Since the densities from Higgs (1971) are model-dependent, we have plotted a similar diagram in Figure 4*b* using electron densities derived from the forbidden line ratio of [O II] λλ3726, 3729 as discussed earlier in the description of column (9) of Table 5. We have excluded BD +30°3639 from Figure 4 for the reasons mentioned earlier.

Inspection of Figure 4*a* shows that a correlation exists between log $\{n_e(\text{rms})\}$ and the log of the ratio of 9.8 μm and 5 GHz fluxes only if those nebulae are included whose values of $L_{IR}/L_{L\alpha}$ indicate direct absorption of stellar photons to be significant. If these nebulae (NGC 6790, NGC 6807, NGC 7027, and IC 5117) are excluded, then a formal least-squares analysis yields a correlation coefficient of $r^2 = 0.04$ for the remaining 21 nebulae. For all 25 nebulae r^2 rises to 0.36. A similar situation holds for the plot of log $\{n_e(\text{FL})\}$ versus the log of the ratio of 9.8 μm and 5 GHz fluxes in Figure 4*b*. For all 17 nebulae, a least-squares analysis yields a correlation coefficient of $r^2 = 0.64$. With the exclusion of NGC 6790 and NGC 7027, r^2 falls to 0.42; and with the additional exclusion of IC 418, r^2 falls to 0.26. We interpret Figures 4*a* and 4*b* as showing that no significant correlation exists between log n_e and log $\{F_\nu(9.8\ \mu\text{m})/F_\nu(5\ \text{GHz})\}$ for nebular electron densities less than $n_e \sim 1.5\text{–}2 \times 10^4$ cm^{-3}, as would be expected on the basis of a model whereby grain heating is powered by Lα photons. When nebulae with $n_e > 1.5 \times 10^4$ cm^{-3} are included, a correlation does exist but these nebulae are precisely the ones whose values of $L_{IR}/L_{L\alpha}$ indicate direct absorption of stellar photons to be important, and thus their inclusion would be expected to yield the observed correlations. When $L_{IR}/L_{L\alpha}$ is plotted against electron density (not shown here), the same conclusions are obtained.

We may therefore outline the following general scenario for the infrared behavior of model planetary nebulae. A young planetary nebula with a high electron density will have a large dust optical depth in the Lyman continuum, τ_{UV}, such that direct grain heating by stellar photons dominates diffuse Lα heating. As the nebula expands, τ_{UV} will fall; e.g., for a uniform density nebula of radius R, $n_e R^3$ is a constant, so for a dust-to-gas ratio which remains constant, $\tau_{UV} \propto n_e R$, implying $\tau_{UV} \propto R^{-2}$. In considering the behavior of the neutral hydrogen optical depth in the Lyman continuum, τ_{H^0}, we may distinguish two cases: (*a*) a density-bounded nebula, and (*b*) a radiation-bounded nebula surrounded by a neutral shell. For

[4] The correlation coefficient

$$r^2 = \frac{[\sum x_i y_i - (\sum x_i \sum y_i/n)]^2}{\{\sum x_i^2 - [(\sum x_i)^2/n]\}\{\sum y_i^2 - [(\sum y_i)^2/n]\}}.$$

case (*a*) of an expanding density-bounded nebula with $\tau_{H^0} = n_{H^0}R$, we have $n_{H^0}R^{-2} \propto n_H n_e$, as ionizations must balance recombinations. Since $n_H \sim n_e \propto R^{-3}$, we thus find that $\tau_{H^0} \propto R^{-3}$. Therefore, as the nebula expands and density decreases, the fraction of photons absorbed by gas will decrease faster than the fraction absorbed by dust and $L_{IR}/L_{L\alpha}$ will increase. For case (*b*) of a radiation-bounded nebula, there will always be sufficient neutral hydrogen surrounding the nebula to absorb the Lyman continuum completely. Therefore, as the dust optical depth falls as the nebula expands, the fraction of the Lyman continuum absorbed by gas will increase and $L_{IR}/L_{L\alpha}$ will decrease. Eventually, at some transition nebular density, direct grain heating by stellar photons will fall below Lα heating and thereafter Lα will dominate. The observations indicate that case (*b*) holds and that the transition nebular density is approximately 1.5×10^4 cm^{-3}. This result is consistent with the fact that planetary nebulae having densities of this order are generally believed to be radiation-bounded. The probability of dust absorption of Lα photons does not fall rapidly with density, since typically a Lα photon must undergo several tens to thousands of H-atom scatterings before escaping from a nebula. A small dust optical depth is therefore sufficient to cause significant absorption of Lα (cf. Panagia and Ranieri 1973). Eventually, however, as the nebula continues to expand, the density will fall to a level where the Lα scattering optical depth is sufficiently low that most Lα photons will escape the nebula without being absorbed, and $L_{IR}/L_{L\alpha}$ will fall once again. It is not possible to estimate this transition density here since the nebular densities encountered in the present sample do not extend below $\sim 2 \times 10^3$ cm^{-3}. It is assumed that planetary nebulae make the transition from being radiation-bounded to being density-bounded at a density far enough below $\sim 1.5 \times 10^4$ cm^{-3} that the effects associated with case (*a*) on $L_{IR}/L_{L\alpha}$, described above, are not noticeable due to the complete dominance of Lα heating.

We have not attempted to make estimates of the mass of dust contained in the planetary nebulae in our sample since, as discussed by Panagia, Bussoletti, and Blanco (1977) and Mathis (1978), such estimates require a knowledge of both the composition of the dust and the grain size distribution. Estimates made without specific knowledge of these parameters are likely to give unreliable results. For instance, the method of Koppen (1977), when applied to the 10 and 30 μm fluxes of NGC 7027, gives estimates of the mass of dust which differ by a factor of 100, whereas the mass of dust estimated for the same nebula by Telesco and Harper (1977), assuming an infrared emissivity appropriate for dielectric grains, would be increased by a factor of about 15 if equally, or more, plausible conducting grains such as graphite were assumed.

In conclusion, we would like to emphasize the importance of far-infrared observations of planetary nebulae at wavelengths longer than 20 μm, both to confirm the present conclusions concerning the transition density from stellar continuum to Lα dominated grain heating, and in order to extend the sample to larger, lower-density nebulae.

We thank D. K. Aitken, D. A. Allen, and P. F. Roche for discussions; J. A. Frogel for his abundant help and advice with the operation of the CTIO infrared equipment; and the Director and staff of CTIO for their hospitality. M. C. thanks the Director and staff of NRAO in Tucson for their hospitality and expertise. M. C. thanks the National Science Foundation for its support of this work under grants AST 75-13511 and AST 77-19896, and the National Research Council for an NAS/NRC Senior Associateship. M. J. B. thanks the National Science Foundation for support under grant AST 76-22032.

REFERENCES

Acker, A. 1978, *Astr. Ap. Suppl.*, **33**, 367.
Aitken, D. K., Roche, P. F., Spenser, P. M., and Jones, B. 1979, *Ap. J.*, **223**, 925.
Allen, D. A. 1973, *M.N.R.A.S.*, **161**, 145.
Allen, D. A., and Swings, J. P. 1976, *Astr. Ap.*, **47**, 293.
Becklin, E. E., Neugebauer, G., and Wynn-Williams, C. G. 1973, *Ap. Letters*, **15**, 87.
Cohen, M., and Barlow, M. J. 1974, *Ap. J.*, **193**, 401 (Paper I).
Danziger, I. J., Frogel, J. A., and Persson, S. E. 1973, *Ap. J. (Letters)*, **184**, L29.
Gehrz, R. D., Hackwell, J. A., and Jones, T. W. 1974, *Ap. J.*, **191**, 675.
Gillett, F. C., Forrest, W. J., and Merrill, K. M. 1973, *Ap. J.*, **183**, 87.
Gillett, F. C., Jones, T. W., Merrill, K. M., and Stein, W. A. 1975, *Astr. Ap.*, **45**, 77.
Grasdalen, G. L. 1979, *Ap. J.*, **229**, 587.
Higgs, L. A. 1971, *Catalog of Radio Observations of Planetary Nebulae and Related Optical Data* (Pub. Ap. Branch, NRC, Canada), Vol. **1**, No. 1.
Koppen, J. 1977, *Astr. Ap.*, **56**, 189.
Marsh, K. A., Purton, C. R., and Feldman, P. A. 1976, *Astr. Ap.*, **49**, 211.
Mathis, J. S. 1978, in *Proc. IAU Symposium 76, Planetary Nebulae Observations and Theory*, ed. Y. Terzian (Dordrecht: Reidel), p. 281.
McCarthy, J. F., Forrest, W. J., and Houck, J. R. 1978, *Ap. J.*, **224**, 109.
Milne, D. K. 1979, *Astr. Ap. Suppl.*, **36**, 227.
Milne, D. K., and Aller, L. H. 1975, *Astr. Ap.*, 38, 183.
O'Dell, C. R., and Terzian, Y. 1970, *Ap. J.*, **160**, 915.
Panagia, N., Bussoletti, E., and Blanco, A. 1977, CNO *Isotopes in Astrophysics*, ed. J. Audouze (Dordrecht: Reidel), p. 45.
Panagia, N., and Ranieri, M. 1973, *18th Liège Colloquium, Les Nébuleuses Planétaires*, p. 275.
Perek, L., and Kohoutek, L. 1967, *Catalogue of Galactic Planetary Nebulae* (Prague: Czechoslovak Institute of Sciences).
Rieke, G. H. 1974, *Ap. J. (Letters)*, **193**, L81.
Rubin, R. H. 1968, *Ap. J.*, **154**, 391.
Russell, R. W., Soifer, B. T., and Willner, S. P. 1977, *Ap. J. (Letters)*, **217**, L149.

Sabbadin, F., and Minello, S. 1978, *Astr. Ap. Suppl.*, **33**, 223.
Sanduleak, N., and Phillip, A. G. Davis. 1977, *Pub. A.S.P.*, **89**, 792.
Sanduleak, N., and Stephenson, C. B. 1972, *Ap. J.*, **178**, 183.
———. 1973, *Ap. J.*, **185**, 899.
Smith, L. F., and Aller, L. H. 1969, *Ap. J.*, **157**, 1245.
Swings, J. P. 1973, *Ap. Letters*, **15**, 71.
Telesco, C. M., and Harper, D. A. 1977, *Ap. J.*, **211**, 475.
Webster, B. L., and Glass, I. S. 1974, *M.N.R.A.S.*, **166**, 491.
Willner, S. P., Jones, B., Puetter, R. C., Russell, R. W., and Soifer, B. T. 1979, preprint.
Wright, A. E., and Barlow, M. J. 1975, *M.N.R.A.S.*, **170**, 41.

MARTIN COHEN: NASA Ames Research Center, Mailstop 245-6, Moffett Field, CA 94035

MICHAEL J. BARLOW: Department of Physics and Astronomy, University College London, Gower Street, London WC1E 6BT, England